

Single G centers in silicon fabricated by co-implantation with carbon and proton

Cite as: Appl. Phys. Lett. **121**, 084003 (2022); doi: [10.1063/5.0097407](https://doi.org/10.1063/5.0097407)

Submitted: 28 April 2022 · Accepted: 5 August 2022 ·

Published Online: 24 August 2022



View Online



Export Citation



CrossMark

Yoann Baron,¹  Alrik Durand,¹  Tobias Herzig,²  Mario Khoury,³ Sébastien Pezzagna,²  Jan Meijer,²  Isabelle Robert-Philip,¹  Marco Abbarchi,³  Jean-Michel Hartmann,⁴ Shay Reboh,⁴  Jean-Michel Gérard,⁵  Vincent Jacques,¹  Guillaume Cassabois,¹  and Anaïs Dréau^{1,a)} 

AFFILIATIONS

¹Laboratoire Charles Coulomb, Université de Montpellier and CNRS, 34095 Montpellier, France

²Division of Applied Quantum Systems, Felix Bloch Institute for Solid State Physics, University Leipzig, Linnéstraße 5, 04103 Leipzig, Germany

³CNRS, Aix-Marseille Université, Centrale Marseille, IM2NP, UMR 7334, Campus de St. Jérôme, 13397 Marseille, France

⁴University Grenoble Alpes and CEA, LETI, F-38000 Grenoble, France

⁵University Grenoble Alpes, CEA, Grenoble INP, IRIG-PHELIQS, F-38000 Grenoble, France

^{a)}Author to whom correspondence should be addressed: anaïs.dreau@umontpellier.fr

ABSTRACT

We report the fabrication of isolated G centers in silicon with single photon emission at optical telecommunication wavelengths. Our sample is made from a silicon-on-insulator wafer, which is locally implanted with carbon ions and protons at various fluences. Decreasing the implantation fluences enables us to gradually switch from large ensembles to isolated single defects, reaching areal densities of G centers down to $\sim 0.2 \mu\text{m}^{-2}$. Single defect creation is demonstrated by photon antibunching in intensity-correlation experiments, thus establishing our approach as an effective procedure for generating single artificial atoms in silicon for future quantum technologies.

Published under an exclusive license by AIP Publishing. <https://doi.org/10.1063/5.0097407>

Silicon is the major semiconductor of the information society. It is at the heart of the devices in microelectronics and computer technology and as such the most desired platform for the development of the next generation applications in quantum technologies. On the one hand, individual dopants^{1,2} and gate-defined quantum dots^{3,4} have already emerged for implementing electrical qubits in silicon. On the other hand, the literature is still very sparse on silicon-based quantum devices harnessing individual optically active qubits for quantum communications and integrated quantum photonics.^{5–7} Recent studies demonstrating the coherent control of fluorescent spin-defects in silicon^{8,9} and the single-photon emission from several families of isolated single near-infrared color centers in silicon^{9–13} could change the game. However, no procedure that permits the reproducible creation of individual optically active artificial atoms with various densities in silicon has been established yet. This capability is essential not only for optical experiments at the single-defect level but also in view of the deterministic integration of an individual color-center in an optical photonic microstructure to build quantum photonic devices.

In this Letter, we report on the fabrication at single-defect scale of the **G center in silicon**, whose emission spectrum is characterized by

a zero-phonon line (ZPL) at 1279 nm matching the O-band of optical telecommunication wavelengths.¹⁴ The microscopic structure of this defect consists of two substitutional carbon atoms connected by an interstitial silicon atom.¹⁵ To create this color center, a silicon-on-insulator (SOI) wafer is locally implanted with carbon ions and irradiated with protons at various fluences in a cross-implantation scheme. Decreasing the implantation fluences enables to gradually switch from dense to dilute arrays, reaching areal densities of G centers down to $\sim 0.2 \mu\text{m}^{-2}$, while keeping the same emission spectra whatever the density. Single defect creation is demonstrated by photon antibunching in intensity-correlation experiments, thus establishing our approach as an effective procedure for generating single artificial atoms in silicon for future quantum technologies.

The investigated wafer consists of a ^{28}Si epilayer grown on a commercial SOI wafer. The advantage of the SOI structure is that it is suitable for integrated quantum photonics. Although isotopic purification plays no role in the present paper, the use of ^{28}Si ensures a nuclear spin-free host matrix¹⁶ for the optically active defects and also a reduced inhomogeneous broadening¹⁷ for future studies. The top Si-layer of the commercial SOI is thinned down to 4 nm by thermal

oxidation, followed by wet hydrofluoric acid chemical etching. The growth of ^{28}Si by chemical vapor deposition is described in Ref. 18. The resulting stack is made of a 56 nm thick layer of ^{28}Si and a 4 nm thick layer of natural Si, that are separated from the substrate by a 145 nm thick layer made of natural silicon oxide. This wafer is then cut into pieces to produce the samples studied here. To create G centers, a first sample (No. 1) is implanted with carbon ions and then irradiated with protons.^{19,20} In between these two implantation processes, this sample is subjected to a flash annealing at 1000 °C during 20 s under N_2 atmosphere^{19,20} in order to heal the silicon lattice from the implantation damage and allow the implanted carbon atoms to move onto substitutional lattice site. To serve as a reference, a second sample (No. 2) is kept in its virgin state, i.e., without any additional step following the ^{28}Si epilayer growth. To analyze the influence of the annealing step, another virgin sample (No. 3) undergoes only the flash annealing without any implantation.

The samples are characterized by spatially resolved photoluminescence (PL) spectroscopy in a scanning confocal microscope built in a closed-cycle He cryostat, as described in Ref. 10. PL detection is performed with superconducting single-photon detectors (SingleQuantum) after a 1050 nm long-pass filter. Without further indications, the data presented here are recorded at 30 K under CW 532 nm excitation at 10 μW .

Before investigating the implanted SOI sample, we first analyze the virgin reference SOI sample and the influence of the flash annealing step. A PL map of the virgin sample No. 2 is displayed in Fig. 1(a). It reveals a spatially uniform background with few hotspots of slightly higher intensity. Their typical PL spectrum is shown in Fig. 1(c): it features a broad PL emission centered at ~ 1350 nm and no ZPL. Such an emission spectrum differs from the one of G centers [see Fig. 2(b)].¹⁹ The presence of native G centers in the pristine SOI wafer studied here can, thus, be ruled out. The impact of the flash annealing at 1000 °C during 20 s under N_2 atmosphere is seen in the PL map of sample No. 3 in Fig. 1(b). The intensity of the spatially uniform PL background is reduced by a factor ~ 2 so that the native hotspots are better resolved. Still, neither the intensity nor the spectrum of their PL signal changes due to the flash annealing step. From this second control experiment, we conclude that flash annealing alone does not contribute to the formation of G centers in silicon. Conversely, all the G centers studied below are the products of the implantation by both carbon ions and protons, especially in the low-density regions of the samples where single G defects are detected.

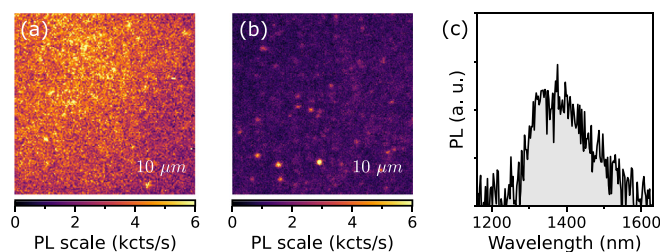


FIG. 1. PL map of (a) the virgin sample (No. 2) and (b) the sample after a flash annealing of 20 s at 1000 °C under N_2 atmosphere (No. 3). (c) Typical PL spectrum of the hotspots in (a) and (b). Data are recorded at 30 K under excitation at 532 nm with an optical power of 10 μW .

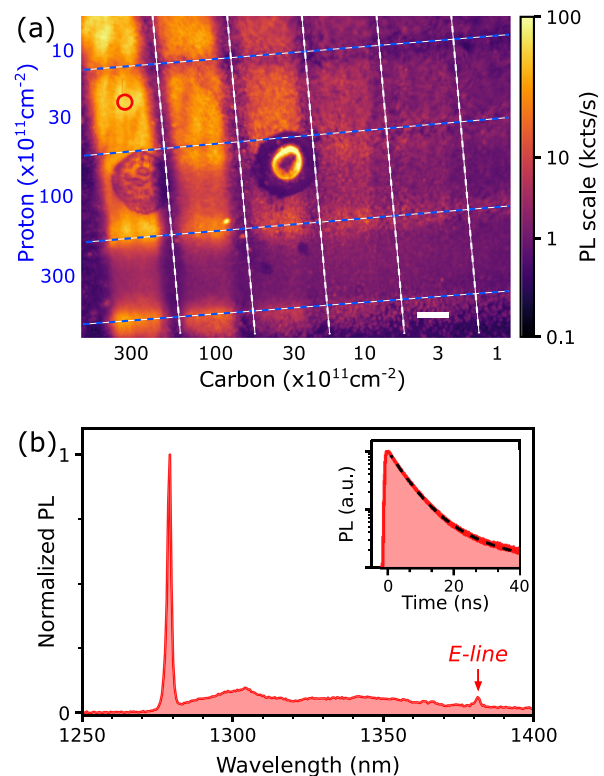


FIG. 2. (a) PL map of the SOI sample (No. 1) cross-implanted with carbon and proton in the region of high irradiation fluences. The vertical white (horizontal blue) dashed lines are guides for the eyes splitting the stripes with different carbon (proton) fluences, whose values are indicated in the bottom (left) axis. The white bar scales for 10 μm . The two 20 μm large spots visible in the left middle of the scan are due to local sample imperfections. (b) PL spectrum detected for an ensemble of G centers at the position indicated by the red circle in (a). These data are recorded at 30 K under excitation at 532 nm with an optical power of 10 μW . Inset: Time-resolved PL decay recorded with a 150 ps pulsed laser at 532 nm. The black dashed line represents data fitting with a bi-exponential function (see main text for details).

Dense ensembles of G centers can be created by implanting crystalline silicon with carbon ions and protons.^{19,20} Our approach consists here in keeping this dual implantation while tuning the areal density of the centers by varying the implantation doses. Localized ion implantation is performed through a 30 μm thick mica mask with a $20 \times 200 \mu\text{m}^2$ aperture on sample No. 1. A 7×7 implantation grid pattern is performed by superimposing seven vertical carbon-implanted stripes with seven horizontal proton-irradiated stripes separated by $\sim 10 \mu\text{m}$. This configuration allows to probe 49 combinations of carbon and proton doses for generating G centers. The fluences vary from 0.3 to $300 \times 10^{11} \text{cm}^{-2}$ for both carbon and proton, which are implanted at energies of 8 and 6 keV, respectively. At these energies, the carbon ions stop in the upper silicon layer whereas the protons cross it while producing interstitials and stop in the oxide layer below (see the [supplementary material](#)).

Figure 2(a) shows the PL intensity map obtained from the most heavily implanted part of our SOI sample. The carbon and proton fluences, indicated along the bottom and left axes, vary from 1 to

$300 \times 10^{11} \text{ cm}^{-2}$. We observe that the sample luminescence varies significantly from one implantation square to another. While the PL signal intensity increases monotonously with the carbon dose (right to left), there is a maximum at $30 \times 10^{11} \text{ cm}^{-2}$ when raising the proton concentration (top to bottom). Above this fluence, the irradiated stripes acquire an inverted contrast in PL mapping with a dark center and bright horizontal edges. This reveals the detrimental effect of the proton irradiation at high fluences to create G centers, as previously observed for silicon wafers highly implanted with carbon ions.²⁰

A PL spectrum recorded in the area with the highest PL intensity is displayed in Fig. 2(b). The sharp ZPL at 1279 nm and the broad phonon-sideband (PSB) at longer wavelengths are characteristic of the G center in silicon, as previously reported in ensemble measurements.¹⁹ Of particular importance is the so-called E-line at 1380 nm, which corresponds to a local vibration mode of the G center and is, thus, a key fingerprint of this point defect.¹⁴ These results are consistent with former works from Refs. 19 and 20 and confirm the effectiveness of this dual carbon and proton implantation method to produce G-center ensembles in a SOI wafer. Time-resolved PL experiments under 150 ps pulsed laser excitation at 532 nm [Fig. 2(b), inset] show that the luminescence decays first with a short constant time of $4.5 \pm 0.1 \text{ ns}$, close to the mono-exponential decay time of $\approx 5.9 \text{ ns}$ reported on dense ensembles of G centers in a 220 nm thick SOI wafer.¹⁹ Nevertheless, we note that the recombination dynamics here involves also a longer decay time of $11.6 \pm 0.2 \text{ ns}$. As discussed in the following, this longer lifetime is presumably associated with other defects emitting in the spectral range of the G center.

Upon decreasing the carbon and proton fluences, the PL signal intensity decreases, as expected for more and more dilute ensembles of fluorescent defects. Figure 3(a) shows a map of the PL signal in the low irradiation region of our cross-implanted SOI. In these areas, the PL signal intensity is no longer spatially uniform featuring separated bright spots whose relative distance increases while decreasing carbon and proton fluences. The PL spectrum of such an isolated spot in the area implanted with carbon and proton, respectively, at 0.3×10^{11} and $1 \times 10^{11} \text{ cm}^{-2}$ is displayed in Fig. 3(c). It is identical to the one previously measured on the ensemble of G centers [Fig. 2(b)], with, in particular, the presence of the E-line at 1381 nm, which allows to attribute it without ambiguity to G center emission. The photon antibunching observed in intensity-correlation experiments with $g^{(2)}(0) < 0.5$ attests that it is a single emitter [Fig. 3(b)],²¹ thus demonstrating the detection of a single G center in silicon. The estimated areal density of fluorescent defects is roughly 0.2 per μm^2 . We highlight the difference with our previous measurements on single defects in silicon^{10,11} where the PL spectrum was never entirely identical to the one of G center ensembles.¹⁹ Besides an average shift of the ZPL of 9 nm toward the lowest wavelengths, the E-line was notably missing for the single defects reported in Refs. 10 and 11, suggesting a perturbed conformation with respect to the G center structure. Identifying this atomic configuration would require further experimental and theory investigations. In these former works, the SOI wafer was full scale implanted with carbon at a fluence of $500 \times 10^{11} \text{ cm}^{-2}$, a high value which appears unfavorable to the formation of “genuine” G centers, i.e., with a ZPL centered onto 1279 nm and the E-line in their PSB. In contrast, the PL spectrum is here exactly the same for ensembles and isolated spots, as seen in Figs. 2(b) and 3(b). PL spectra have been recorded on about 30 isolated hotspots in this low irradiation region, and they are all associated with G center emission.

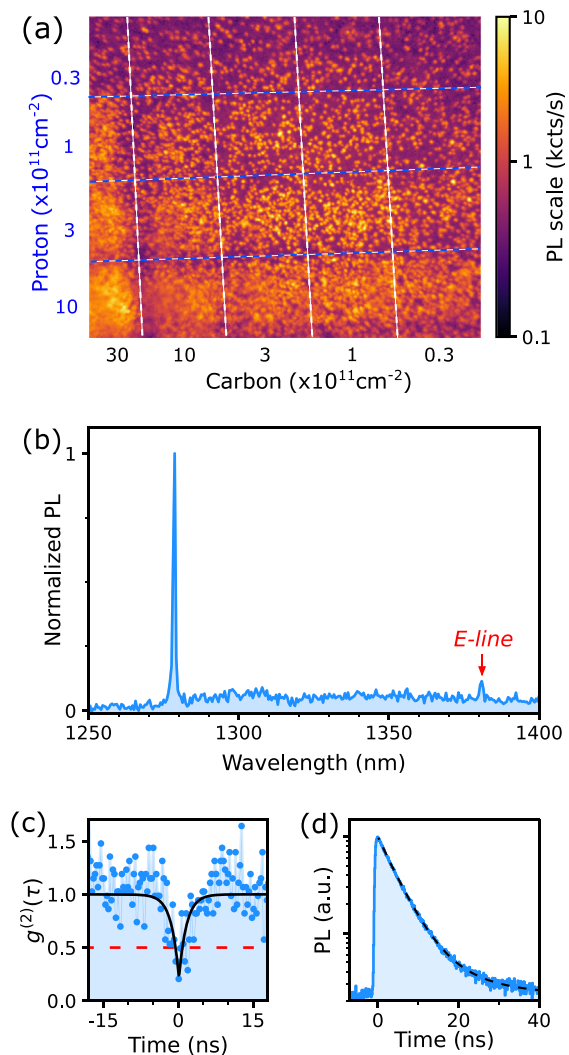


FIG. 3. (a) PL map of the SOI sample No. 1 in the region of low irradiation fluences. The vertical white (horizontal blue) dashed lines are guides for the eyes splitting the stripes with different carbon (proton) fluences, whose value is indicated in the bottom (left) axis. The white bar scales for $10 \mu\text{m}$. (b) PL spectrum detected for an isolated G center indicated by the blue circle in (a). (c) Corresponding intensity-correlation function $g^{(2)}(\tau)$, without any correction from background or detector noise counts. The photon antibunching with $g^{(2)}(0) < 0.5$ evidences the emission of single photons. These data are recorded at 30 K under excitation at 532 nm with an optical power of $10 \mu\text{W}$. (d) Time-resolved PL trace for this single G center acquired with a 150 ps 532 nm pulsed laser.

We have, thus, achieved the regime of single G centers in the dilute regions of the cross-implanted SOI, thereby establishing the effectiveness of this approach to produce large numbers of isolated G centers in silicon devices.

To probe the recombination dynamics, time-resolved PL measurements under pulsed-laser excitation are reproduced on single G centers. As displayed in Fig. 3(d), the PL signal decay is mainly mono-exponential with more than 80% of the photons linked to a timescale of $4.5 \pm 0.1 \text{ ns}$, identical to the short lifetime previously measured on

the G-center ensemble [Fig. 2(b), inset]. The remaining of the photons are associated with a decay time of 12 ± 3 ns. Unlike the 4.5-ns time, this long decay time is still observed by repeating the experiment a few micrometers away from the PL isolated hotspots, suggesting that it results from sample PL background. The slight difference in the G-center excited-state lifetime measured here and in a former sample [≈ 5.9 ns (Ref. 19)] could be linked to a change in the thickness of the SOI stack layers.²² Complementary experiments will be required to further elucidate the recombination dynamics of the G center in silicon and identify its intrinsic channels.

In summary, we report the generation of single G centers in silicon by co-implantation with carbon ions and protons. Control experiments in the SOI wafer either pristine or after only flash annealing at 1000 °C rule out the existence of native centers or their creation by the flash annealing step. G centers are solely generated by carbon and proton implantation. Decreasing the implantation fluences leads to the fabrication of dilute arrays of centers down to areal densities compatible with single photon emission in the telecom O-band. The PL spectra are identical in ensembles of centers and in single G centers, establishing of an effective procedure for the creation of single centers in silicon for future quantum technologies.

Note added in proof: After submission of this manuscript, we have been aware of a related work by Hollenbach *et al.*,²³ which reports the fabrication of single G centers in silicon using silicon focused-ion beam on carbon-doped silicon samples.

See the [supplementary material](#) for additional information on stopping and range of ions in matter (SRIM) simulation data for the carbon and proton implantations.

This work was supported by the French National Research Agency (ANR) through the projects ULYSSES (No. ANR-15-CE24-0027-01), OCTOPUS (No. ANR-18-CE47-0013-01), and QUASSIC (No. ANR-18-ERC2-0005-01), the Occitanie region through the SITEQ contract, the German Research Foundation (DFG) through the ULYSSES project (No. PE 2508/1-1), and the European Union's Horizon 2020 program through the FET-OPEN project NARCISO (No. 828890) and the ASTERISQ project (Grant No. 820394). The authors thank the Nanotecmat platform of the IM2NP institute and Louis Hutin and Benoît Bertrand (CEA Leti) for their contributions to the preparation of the ²⁸SOI substrates. A. Durand acknowledges support from the French DGA.

AUTHOR DECLARATIONS

Conflict of Interest

The authors have no conflicts to disclose.

Author Contributions

Yoann Baron: Investigation (lead); Software (lead); Visualization (lead); Writing – review and editing (lead). **Shay Reboh:** Resources (lead); Writing – review and editing (supporting). **Jean-Michel Gérard:** Resources (lead); Writing – original draft (lead); Writing – review and editing (lead). **Vincent Jacques:** Supervision (equal); Writing – review and editing (lead). **Guillaume Cassabois:** Supervision (equal); Writing – original draft (lead); Writing – review and editing (lead). **Anais Dréau:** Supervision (lead); Visualization

(lead); Writing – original draft (lead); Writing – review and editing (lead). **Alrik Durand:** Investigation (lead); Software (lead); Visualization (equal); Writing – review and editing (lead). **Tobias Herzog:** Resources (lead); Writing – review and editing (equal). **Mario Khoury:** Resources (equal); Writing – review and editing (supporting). **Sebastien Pezzagna:** Resources (lead); Writing – review and editing (equal). **Jan Meijer:** Resources (supporting); Writing – review and editing (supporting). **Isabelle Robert-Philip:** Writing – review and editing (lead). **Marco Abbarchi:** Resources (equal); Writing – review and editing (equal). **Jean-Michel Hartmann:** Resources (lead); Writing – review and editing (supporting).

DATA AVAILABILITY

The data that support the findings of this study are available from the corresponding author upon reasonable request.

REFERENCES

- Y. He, S. K. Gorman, D. Keith, L. Kranz, J. G. Keizer, and M. Y. Simmons, “A two-qubit gate between phosphorus donor electrons in silicon,” *Nature* **571**, 371–375 (2019).
- A. Morello, J. J. Pla, P. Bertet, and D. N. Jamieson, “Donor spins in silicon for quantum technologies,” *Adv. Quantum Technol.* **3**, 2000005 (2020).
- T. F. Watson, S. G. J. Philips, E. Kawakami, D. R. Ward, P. Scarlino, M. Veldhorst, D. E. Savage, M. G. Lagally, M. Friesen, S. N. Coppersmith, M. A. Eriksson, and L. M. K. Vandersypen, “A programmable two-qubit quantum processor in silicon,” *Nature* **555**, 633–637 (2018).
- A. M. J. Zwerver, T. Krähenmann, T. F. Watson, L. Lampert, H. C. George, R. Pillarisetty, S. A. Bojarski, P. Amin, S. V. Amitonov, J. M. Boter, R. Caudillo, D. Corras-Serrano, J. P. Dehollain, G. Droulers, E. M. Henry, R. Kotlyar, M. Lodari, F. Lüthi, D. J. Michalak, B. K. Mueller, S. Neyens, J. Roberts, N. Samkharadze, G. Zheng, O. K. Zietz, G. Scappucci, M. Veldhorst, L. M. K. Vandersypen, and J. S. Clarke, “Qubits made by advanced semiconductor manufacturing,” *Nat. Electron.* **5**, 184–190 (2022).
- S. Simmons, “A single silicon colour centre resolved,” *Nat. Electron.* **3**, 734–735 (2020).
- G. Zhang, Y. Cheng, J.-P. Chou, and A. Gali, “Material platforms for defect qubits and single-photon emitters,” *Appl. Phys. Rev.* **7**, 031308 (2020).
- M. Prabhu, C. Errando-Herranz, L. De Santis, I. Christen, C. Chen, and D. R. Englund, “Individually addressable artificial atoms in silicon photonics,” *arXiv:2202.02342* (2022).
- L. Bergeron, C. Chartrand, A. T. K. Kurkjian, K. J. Morse, H. Riemann, N. V. Abrosimov, P. Becker, H.-J. Pohl, M. L. W. Thewalt, and S. Simmons, “Silicon-integrated telecommunications photon-spin interface,” *PRX Quantum* **1**, 020301 (2020).
- D. B. Higginbottom, A. T. K. Kurkjian, C. Chartrand, M. Kazemi, N. A. Brunelle, E. R. MacQuarrie, J. R. Klein, N. R. Lee-Hone, J. Stacho, M. Ruether, C. Bowness, L. Bergeron, A. DeAbreu, S. R. Harrigan, J. Kanaganayagam, D. W. Marsden, T. S. Richards, L. A. Stott, S. Roorda, K. J. Morse, M. L. W. Thewalt, and S. Simmons, “Optical observation of single spins in silicon,” *Nature* **607**, 266–270 (2022).
- W. Redjem, A. Durand, T. Herzog, A. Benali, S. Pezzagna, J. Meijer, A. Y. Kuznetsov, H. S. Nguyen, S. Cuffé, J.-M. Gérard, I. Robert-Philip, B. Gil, D. Caliste, P. Pochet, M. Abbarchi, V. Jacques, A. Dréau, and G. Cassabois, “Single artificial atoms in silicon emitting at telecom wavelengths,” *Nat. Electron.* **3**, 738–743 (2020).
- A. Durand, Y. Baron, W. Redjem, T. Herzog, A. Benali, S. Pezzagna, J. Meijer, A. Kuznetsov, J.-M. Gérard, I. Robert-Philip, M. Abbarchi, V. Jacques, G. Cassabois, and A. Dréau, “Broad diversity of near-infrared single-photon emitters in silicon,” *Phys. Rev. Lett.* **126**, 083602 (2021).
- M. Hollenbach, Y. Berencén, U. Kentsch, M. Helm, and G. V. Astakhov, “Engineering telecom single-photon emitters in silicon for scalable quantum photonics,” *Opt. Express* **28**, 26111–26121 (2020).

- ¹³Y. Baron, A. Durand, P. Udvarhelyi, T. Herzig, M. Khoury, S. Pezzagna, J. Meijer, I. Robert-Philip, M. Abbarchi, J.-M. Hartmann, V. Mazzocchi, J.-M. Gérard, A. Gali, V. Jacques, G. Cassaboïs, and A. Dréau, "Detection of single W-centers in silicon," *ACS Photonics* **9**, 2337 (2022).
- ¹⁴G. Davies, "The optical properties of luminescence centres in silicon," *Phys. Rep.* **176**, 83–188 (1989).
- ¹⁵P. Udvarhelyi, B. Somogyi, G. Thiering, and A. Gali, "Identification of a telecom wavelength single photon emitter in silicon," *Phys. Rev. Lett.* **127**, 196402 (2021).
- ¹⁶K. Saeedi, S. Simmons, J. Z. Salvail, P. Dluhy, H. Riemann, N. V. Abrosimov, P. Becker, H.-J. Pohl, J. J. L. Morton, and M. L. W. Thewalt, "Room-temperature quantum bit storage exceeding 39 minutes using ionized donors in silicon-28," *Science* **342**, 830–833 (2013).
- ¹⁷C. Chartrand, L. Bergeron, K. J. Morse, H. Riemann, N. V. Abrosimov, P. Becker, H.-J. Pohl, S. Simmons, and M. L. W. Thewalt, "Highly enriched ²⁸Si reveals remarkable optical linewidths and fine structure for well-known damage centers," *Phys. Rev. B* **98**, 195201 (2018).
- ¹⁸V. Mazzocchi, P. G. Sennikov, A. D. Bulanov, M. F. Churbanov, B. Bertrand, L. Hutin, J. P. Barnes, M. N. Drozdov, J. M. Hartmann, and M. Sanquer, "99.992% ²⁸Si CVD-grown epilayer on 300 mm substrates for large scale integration of silicon spin qubits," *J. Cryst. Growth* **509**, 1–7 (2019).
- ¹⁹C. Beaufils, W. Redjem, E. Rousseau, V. Jacques, A. Y. Kuznetsov, C. Raynaud, C. Voisin, A. Benali, T. Herzig, S. Pezzagna, J. Meijer, M. Abbarchi, and G. Cassaboïs, "Optical properties of an ensemble of G-centers in silicon," *Phys. Rev. B* **97**, 035303 (2018).
- ²⁰D. D. Berhanuddin, M. A. Lourenço, R. M. Gwilliam, and K. P. Homewood, "Co-implantation of carbon and protons: An integrated silicon device technology compatible method to generate the lasing G-center," *Adv. Funct. Mater.* **22**, 2709–2712 (2012).
- ²¹A. Beveratos, S. Kühn, R. Brouri, T. Gacoin, J.-P. Poizat, and P. Grangier, "Room temperature stable single-photon source," *Eur. Phys. J. D* **18**, 191–196 (2002).
- ²²S. T. Ho, S. L. McCall, and R. E. Slusher, "Spontaneous emission from excitons in thin dielectric layers," *Opt. Lett.* **18**, 909–911 (1993).
- ²³M. Hollenbach, N. Klingner, N. S. Jagtap, L. Bischoff, C. Fowley, U. Kentsch, G. Hlawacek, A. Erbe, N. V. Abrosimov, M. Helm, Y. Berencén, and G. V. Astakhov, "Wafer-scale nanofabrication of telecom single-photon emitters in silicon," *arXiv:2204.13173* (2022).